GEOARCHAEOLOGICAL XRF LAB

GEOARCHAEOLOGICAL X-RAY FLUORESCENCE SPECTROMETRY LABORATORY
8100 WYOMING BLVD., SUITE M4-158 ALBUQUERQUE, NM 87113 USA

SOURCE PROVENANCE OF OBSIDIAN ARTIFACTS FROM ARCHAIC SITES IN THE NORTHERN SEA OF CORTEZ, MEXICO

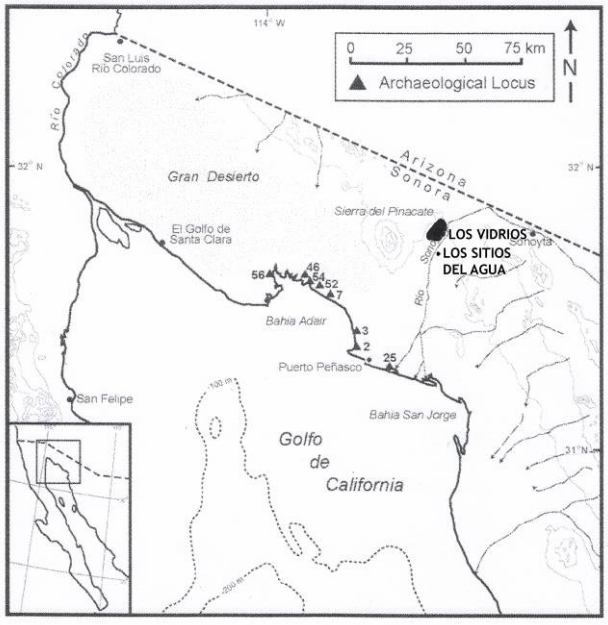

by

M. Steven Shackley Ph.D., Director
Geoarchaeological XRF Laboratory
Albuquerque, New Mexico

Report Prepared for

Doug Mitchell
Scottsdale, Arizona

31 July 2015

INTRODUCTION

The analysis here of 31 obsidian artifacts indicates a relatively diverse assemblage. While most of the artifacts were produced from known sources in the northern Sonoran Desert, a substantial proportion were produced from two, as yet, unlocated sources likely in the region of the northern state of Sonora, Mexico, and never seen before north of the U.S.-Mexico border, indeed anywhere.

LABORATORY SAMPLING, ANALYSIS AND INSTRUMENTATION

All archaeological samples are analyzed whole. The results presented here are quantitative in that they are derived from "filtered" intensity values ratioed to the appropriate x-ray continuum regions through a least squares fitting formula rather than plotting the proportions of the net intensities in a ternary system (McCarthy and Schamber 1981; Schamber 1977). Or more essentially, these data through the analysis of international rock standards, allow for inter-instrument comparison with a predictable degree of certainty (Hampel 1984; Shackley 2011).

Trace Element Analyses

All analyses for this study were conducted on a ThermoScientific *Quant'X* EDXRF spectrometer, located in the Geoarchaeological XRF Laboratory, Albuquerque, New Mexico. It is equipped with a thermoelectrically Peltier cooled solid-state Si(Li) X-ray detector, with a 50 kV, 50 W, ultra-high-flux end window bremsstrahlung, Rh target X-ray tube and a 76 μm (3 mil) beryllium (Be) window (air cooled), that runs on a power supply operating 4-50 kV/0.02-1.0 mA at 0.02 increments. The spectrometer is equipped with a 200 l min^{-1} Edwards vacuum pump, allowing for the analysis of lower-atomic-weight elements between sodium (Na) and titanium (Ti). Data acquisition is accomplished with a pulse processor and an analogue-to-digital converter. Elemental composition is identified with digital filter background removal, least

squares empirical peak deconvolution, gross peak intensities and net peak intensities above background.

The analysis for mid Zb condition elements Ti-Nb, Pb, Th, the x-ray tube is operated at 30 kV, using a 0.05 mm (medium) Pd primary beam filter in an air path at 200 seconds livetime to generate x-ray intensity Ka-line data for elements titanium (Ti), manganese (Mn), iron (as $Fe_2O_3^T$), cobalt (Co), nickel (Ni), copper, (Cu), zinc, (Zn), gallium (Ga), rubidium (Rb), strontium (Sr), yttrium (Y), zirconium (Zr), niobium (Nb), lead (Pb), and thorium (Th). Not all these elements are reported since their values in many volcanic rocks are very low. Trace element intensities were converted to concentration estimates by employing a least-squares calibration line ratioed to the Compton scatter established for each element from the analysis of international rock standards certified by the National Institute of Standards and Technology (NIST), the US. Geological Survey (USGS), Canadian Centre for Mineral and Energy Technology, and the Centre de Recherches Pétrographiques et Géochimiques in France (Govindaraju 1994). Line fitting is linear (XML) for all elements but Fe where a derivative fitting is used to improve the fit for iron and thus for all the other elements. When barium (Ba) is analyzed in the High Zb condition, the Rh tube is operated at 50 kV and up to 1.0 mA, ratioed to the bremsstrahlung region (see Davis 2011; Shackley 2011). Further details concerning the petrological choice of these elements in Southwest obsidians is available in Shackley (1988, 1995, 2005; also Mahood and Stimac 1991; and Hughes and Smith 1993). Nineteen specific pressed powder standards are used for the best fit regression calibration for elements Ti-Nb, Pb, Th, and Ba, include G-2 (basalt), AGV-2 (andesite), GSP-2 (granodiorite), SY-2 (syenite), BHVO-2 (hawaiite), STM-1 (syenite), QLO-1 (quartz latite), RGM-1 (obsidian), W-2 (diabase), BIR-1 (basalt), SDC-1 (mica schist), TLM-1 (tonalite), SCO-1 (shale), NOD-A-1 and NOD-P-1 (manganese) all US Geological Survey standards, NIST-278 (obsidian), U.S. National Institute

of Standards and Technology, BE-N (basalt) from the Centre de Recherches Pétrographiques et Géochimiques in France, and JR-1 and JR-2 (obsidian) from the Geological Survey of Japan (Govindaraju 1994).

The data from the WinTrace software were translated directly into Excel for Windows software for manipulation and on into SPSS for Windows (ver. 21) for statistical analyses. In order to evaluate these quantitative determinations, machine data were compared to measurements of known standards during each run. RGM-1 a USGS obsidian standard is analyzed during each sample run for obsidian artifacts to check machine calibration (Table 1). Source assignments were made by reference to Hinojosa-Prieto (2015); Martynec et al. (2011) and Shackley (1995, 2005 and updated at http://swxrflab.net/swobsrcs.htm; see Tables 1 and 2 and Figure 1.

Major and Minor Oxide Analysis

The group of unknown samples were subjected to major and minor oxide analyses to determine rock type for future research. The two well known sources in northern Sonora, Los Sitios del Agua and Los Vidrios are Tertiary rhyolites as part of the bimodal Sierra Pinacate Volcanic Field. The oxide analysis determined whether the "unknowns" were also rhyolites, possibly related to the Sierra Pinacate field (Table 3 and Figure 3).

Analysis of the major oxides of Si, Al, Ca, Fe, K, Mg, Mn, Na, and Ti is performed under the multiple conditions elucidated below. This fundamental parameter analysis (theoretical with standards), while not as accurate as destructive analyses (pressed powder and fusion disks) is usually within a few percent of actual, based on the analysis of USGS RGM-1 obsidian standard (see also Shackley 2011). The fundamental parameters (theoretical) method is run under conditions commensurate with the elements of interest and calibrated with 11 USGS standards (RGM-1, rhyolite; AGV-2, andesite; BHVO-1, hawaiite; BIR-1, basalt; G-2, granite; GSP-2,

granodiorite; BCR-2, basalt; W-2, diabase; QLO-1, quartz latite; STM-1, syenite), and one Japanese Geological Survey rhyolite standard (JR-1). See Lundblad et al. (2011) for another set of conditions and methods for oxide analyses.

CONDITIONS OF FUNDAMENTAL PARAMETER ANALYSIS[1]

Low Za (Na, Mg, Al, Si, P)

Voltage	6 kV	Current	Auto[2]
Livetime	100 seconds	Counts Limit	0
Filter	No Filter	Atmosphere	Vacuum
Maximum Energy	10 keV	Count Rate	Low

Mid Zb (K, Ca, Ti, V, Cr, Mn, Fe)

Voltage	32 kV	Current	Auto
Livetime	100 seconds	Counts Limit	0
Filter	Pd (0.06 mm)	Atmosphere	Vacuum
Maximum Energy	40 keV	Count Rate	Medium

High Zb (Sn, Sb, Ba, Ag, Cd)

Voltage	50 kV	Current	Auto
Livetime	100 seconds	Counts Limit	0
Filter	Cu (0.559 mm)	Atmosphere	Vacuum
Maximum Energy	40 keV	Count Rate	High

Low Zb (S, Cl, K, Ca)

Voltage	8 kV	Current	Auto
Livetime	100 seconds	Counts Limit	0
Filter	Cellulose (0.06 mm)	Atmosphere	Vacuum
Maximum Energy	10 keV	Count Rate	Low

[1] Multiple conditions designed to ameliorate peak overlap identified with digital filter background removal, least squares empirical peak deconvolution, gross peak intensities and net peak intensities above background.

[2] Current is set automatically based on the mass absorption coefficient.

DISCUSSION

This is the first relatively large scale analysis of archaeological obsidian from the northern Sea of Cortez to my knowledge. While the presence of Los Vidrios and Los Sitios del Agua sources that are just upstream along the Rio Sonoyta from these sites is expectable, the artifacts produced from the, as yet, unlocated sources is new (Shackley 1995, 2005; see Figure 2 here). They are certainly rhyolite glasses as seen on the TAS plot (see Table 3 and Figure 3). Given that most of these "unknown" location obsidian cores and debitage exhibit cortical material, I would predict that they are relatively nearby, and likely part of the bimodal Sierra Pinacate Volcanic Field (Donnely 1974; Gunderson et al. 1986; Gutmann et al. 2000). Some of these samples have relatively high alkalis typical of the mafic volcanics in northwest Mexico, which could also indicate genetic similarity (Gunderson et al. 1986). The rhyolites of the Sierra Pinacate region have not been studied extensively, so more solid inferences are not possible at this time.

The other surprise, was the one artifact produced from the Sauceda Mountains source located north of Ajo, Arizona on the Barry Goldwater Air Force Range in Maricopa County (Sample 5, SON:8:5:7; Table 1). As far as I know, this is the first evidence of an artifact produced from an obsidian source located north of the border down in Sonoran sites. This suggests that these Archaic fisher-gatherers had a somewhat extensive procurement range, not uncommon among Archaic hunter-gatherers in the Southwest (Shackley 1989, 1996).

REFERENCES CITED

Davis, K.D., T.L. Jackson, M.S. Shackley, T. Teague, and J.H. Hampel
2011 Factors Affecting the Energy-Dispersive X-Ray Fluorescence (EDXRF) Analysis of Archaeological Obsidian. In *X-Ray Fluorescence Spectrometry (XRF) in Geoarchaeology*, edited by M.S. Shackley, pp. 45-64. Springer, New York.

Donnely, M.F.
1974 *Geology of the Sierra Pinacate Volcanic Field, Northern Sonora, Mexico and Southern Arizona.* Unpublished Ph.D. dissertation, Department of Geology, Stanford University.

Govindaraju, K.
1994 1994 Compilation of Working Values and Sample Description for 383 Geostandards. *Geostandards Newsletter* 18 (special issue).

Gunderson, R., K. Cameron, and M. Cameron
1986 Cenozoic High-K Calc-Alkalic and Alkalic Volcanism in Eastern Chihuahua, Mexico: Geology and Geochemistry of the Benevides-Pozos Area. *Geological Society of America Bulletin* 97:737-753.

Gutmann, J.T., B.D. Turrin, and J.C. Dohrenwend
2000 Basaltic Rocks from the Pinacate Volcanic Field Yield Notably Young $^{40}Ar/^{39}Ar$ Ages. *Eos: Transactions of the American Geophysical Union* 81:33-37.

Hampel, Joachim H.
1984 Technical Considerations in X-ray Fluorescence Analysis of Obsidian. In *Obsidian Studies in the Great Basin*, edited by R.E. Hughes, pp. 21-25. Contributions of the University of California Archaeological Research Facility 45. Berkeley.

Hildreth, W.
1981 Gradients in Silicic Magma Chambers: Implications for Lithospheric Magmatism. *Journal of Geophysical Research* 86:10153-10192.

Hinojosa-Prieto, H.R., K.W. Kibler, M.S. Shackley, and H.J. Hinojosa-García
2015 The Selene Obsidian Source (Formerly Sonora Unknown B) of the Upper Río Bavispe Basin, Sonora, Mexico. *Kiva*, in press.

Hughes, Richard E., and Robert L. Smith
1993 Archaeology, Geology, and Geochemistry in Obsidian Provenance Studies. *In Scale on Archaeological and Geoscientific Perspectives*, edited by J.K. Stein and A.R. Linse, pp. 79-91. Geological Society of America Special Paper 283.

Lundblad, S.P., P.R. Mills, A. Drake-Raue, and S. K. Kikiloi
2011 Non-Destructive EDXRF Analysis of Archaeological Basalts. In *X-Ray Fluorescence Spectrometry (XRF) in Geoarchaeology*, edited by M.S. Shackley, pp. 65-80. Springer, New York.

Mahood, Gail A., and James A. Stimac
1990 Trace-Element Partitioning in Pantellerites and Trachytes. *Geochemica et Cosmochimica Acta* 54:2257- 2276.

McCarthy, J.J., and F.H. Schamber
1981 Least-Squares Fit with Digital Filter: A Status Report. In *Energy Dispersive X-ray Spectrometry*, edited by K.F.J. Heinrich, D.E. Newbury, R.L. Myklebust, and C.E. Fiori, pp. 273-296. National Bureau of Standards Special Publication 604, Washington, D.C.

Mitchell, D.R., G. Huckleberry, K. Rowell, and D. L. Dettman
2015 Coastal Adaptations During the Archaic Period in the Northern Sea of Cortez, Mexico. *Journal of Island and Coastal Archaeology*, 00:1-24.

Schamber, F.H.
1977 A Modification of the Linear Least-Squares Fitting Method which Provides Continuum Suppression. In *X-ray Fluorescence Analysis of Environmental Samples*, edited by T.G. Dzubay, pp. 241-257. Ann Arbor Science Publishers.

Shackley, M. Steven
1988 Sources of Archaeological Obsidian in the Southwest: An Archaeological, Petrological, and Geochemical Study. *American Antiquity* 53(4):752-772.

1989 *Early Hunter-Gatherer Procurement Ranges in the Southwest: Evidence from Obsidian Geochemistry and Lithic Technology*. Unpublished Ph.D. dissertation, Department of Anthropology, Arizona State University.

1995 Sources of Archaeological Obsidian in the Greater American Southwest: An Update and Quantitative Analysis. *American Antiquity* 60(3):531-551.

1996 Range and Mobility in the Early Hunter-Gatherer Southwest. In *Early Formative Adaptations in the Southern Southwest*, edited by Barbara Roth, pp. 5-16. Monographs in World Prehistory 25. Prehistory Press, Madison.

1998 Intrasource Chemical Variability and Secondary Depositional Processes in Sources of Archaeological Obsidian: Lessons from the American Southwest. In *Archaeological Obsidian Studies: Method and Theory*, edited by M.S. Shackley, pp. 83-102. Advances in Archaeological and Museum Studies 3. Springer, New York.

2005 *Obsidian: Geology and Archaeology in the North American Southwest*. University of Arizona Press, Tucson.

2011 An Introduction to X-Ray Fluorescence (XRF) Analysis in Archaeology. In *X-Ray Fluorescence Spectrometry (XRF) in Geoarchaeology*, edited by M.S. Shackley, pp. 7-44. Springer, New York.

Table 1. Elemental concentrations and source assignments for the archaeological specimens by site, and USGS RGM-1 obsidian standard. All measurements in parts per million (ppm).

Sample	Site	Ti	Mn	Fe	Zn	Rb	Sr	Y	Zr	Nb	SOURCE
1	SON:B:5:7	576	236	12498	96	228	15	67	211	27	Los Vidrios
2	SON:B:5:7	3306	440	21532	83	115	140	41	396	6	SON Unknown C
4	SON:B:5:7	1981	323	17383	66	112	77	45	431	7	SON Unknown D
5	SON:B:5:7	1627	295	12623	60	159	107	25	179	20	Sauceda Mtns
6	SON:B:5:7	567	242	12823	96	243	16	72	219	28	Los Vidrios
7	SON:B:5:7	560	229	12516	86	229	15	67	213	30	Los Vidrios
8	SON:B:5:7	3359	436	21727	102	112	135	46	388	2	SON Unknown C
16	SON:B:5:7	3622	474	22173	100	114	144	44	399	13	SON Unknown C
22	SON:B:5:7	1188	489	20701	191	144	14	83	703	51	Los Sitios del Agua
40	SON:B:5:7	1399	485	20947	188	140	16	80	698	48	Los Sitios del Agua
51	SON:B:5:7	3724	489	24046	104	92	134	43	396	6	SON Unknown C
67	SON:B:5:8	1190	503	21031	174	147	14	89	736	46	Los Sitios del Agua
77	SON:B:11:1	645	228	13070	136	240	16	69	216	30	Los Vidrios
80-1	SON:B:11:1	648	251	13277	112	248	16	69	218	29	Los Vidrios
80-2	SON:B:11:1	637	255	13500	165	249	17	66	219	28	Los Sitios del Agua
87-1	SON:B:11:1	1398	457	20278	174	137	19	79	683	53	Los Vidrios
87-2	SON:B:11:1	615	229	13006	112	242	14	69	216	31	Los Vidrios
87-3	SON:B:11:1	3918	558	24680	122	93	131	43	406	7	SON Unknown C
97	SON:B:11:1	1543	282	14024	359	218	14	53	172	23	Los Vidrios
115-1	SON:B:11:1	778	268	14113	127	264	15	74	231	33	Los Vidrios
115-2	SON:B:11:1	618	240	12922	105	236	14	71	215	30	Los Vidrios
115-3	SON:B:11:1	638	251	13024	114	236	16	68	214	31	Los Vidrios
115-4	SON:B:11:1	643	245	13620	167	251	14	73	219	35	Los Vidrios
115-5	SON:B:11:1	657	238	12719	155	227	16	62	207	33	Los Vidrios
115-6	SON:B:11:1	899	252	13267	163	239	15	65	206	33	Los Vidrios
129	SON:B:11:1	665	254	13540	145	249	15	69	218	28	Los Vidrios

133	SON:B:11:1	757	262	13756	142	258	16	71	223	30	Los Vidrios
136	SON:B:11:1	786	253	13395	173	244	19	67	222	26	Los Vidrios
156	SON:B:11:1	650	236	12858	96	241	14	74	217	31	Los Vidrios
157-1	SON:B:11:1	681	252	13393	91	257	17	75	227	30	Los Vidrios
157-2	SON:B:11:1	4528	576	27503	130	104	141	48	409	9	SON Unknown C
RGM1-S4		1488	282	13711	34	146	105	26	214	10	standard
RGM1-S4		1500	281	13725	38	146	105	26	216	7	standard

Table 2. Crosstabulation of site by source.

			Site			
			SON:B:11:1	SON:B:5:7	SON:B:5:8	Total
SOURCE	Los Sitios del Agua	Count	1	2	1	4
		% within SOURCE	25.0%	50.0%	25.0%	100.0%
		% within Site	5.3%	18.2%	100.0%	12.9%
		% of Total	3.2%	6.5%	3.2%	12.9%
	Los Vidrios	Count	16	3	0	19
		% within SOURCE	84.2%	15.8%	0.0%	100.0%
		% within Site	84.2%	27.3%	0.0%	61.3%
		% of Total	51.6%	9.7%	0.0%	61.3%
	Sauceda Mtns	Count	0	1	0	1
		% within SOURCE	0.0%	100.0%	0.0%	100.0%
		% within Site	0.0%	9.1%	0.0%	3.2%
		% of Total	0.0%	3.2%	0.0%	3.2%
	SON Unknown C	Count	2	4	0	6
		% within SOURCE	33.3%	66.7%	0.0%	100.0%
		% within Site	10.5%	36.4%	0.0%	19.4%
		% of Total	6.5%	12.9%	0.0%	19.4%
	SON Unknown D	Count	0	1	0	1
		% within SOURCE	0.0%	100.0%	0.0%	100.0%
		% within Site	0.0%	9.1%	0.0%	3.2%
		% of Total	0.0%	3.2%	0.0%	3.2%
Total		Count	19	11	1	31
		% within SOURCE	61.3%	35.5%	3.2%	100.0%
		% within Site	100.0%	100.0%	100.0%	100.0%
		% of Total	61.3%	35.5%	3.2%	100.0%

Table 3. Major and minor oxides for the "unknown" samples, and RGM-1 USGS rhyolite standard.

Sample	Site	Na_2O	MgO	Al_2O_3	SiO_2	K_2O	CaO	TiO_2	MnO	Fe_2O_3
		%	%	%	%	%	%	%	%	%
51	SON B:5:7	3.835	0.758	8.377	71.71	5.676	5.779	1.287	0.17	11.193
4	SON B:5:7	3.878	2.883	12.629	72	3.553	1.675	0.403	0.052	3.487
2	SON B:5:7	2.985	0.11	8.539	72.1	6.16	5.572	1.465	0.18	11.627
16	SON B:5:7	3.582	0.667	8.204	68.8	6.38	6.105	1.545	0.206	13.073
87-3	SON B:11-1	3.573	0.377	8.099	71.2	6.328	5.833	1.412	0.198	11.626
157-2	SON B:11-1	4.448	0.453	7.848	69.3	5.661	7.087	1.382	0.178	12.138
RGM1-S4		4.121	0	12.947		4.834	1.387	0.273	0.044	2.195

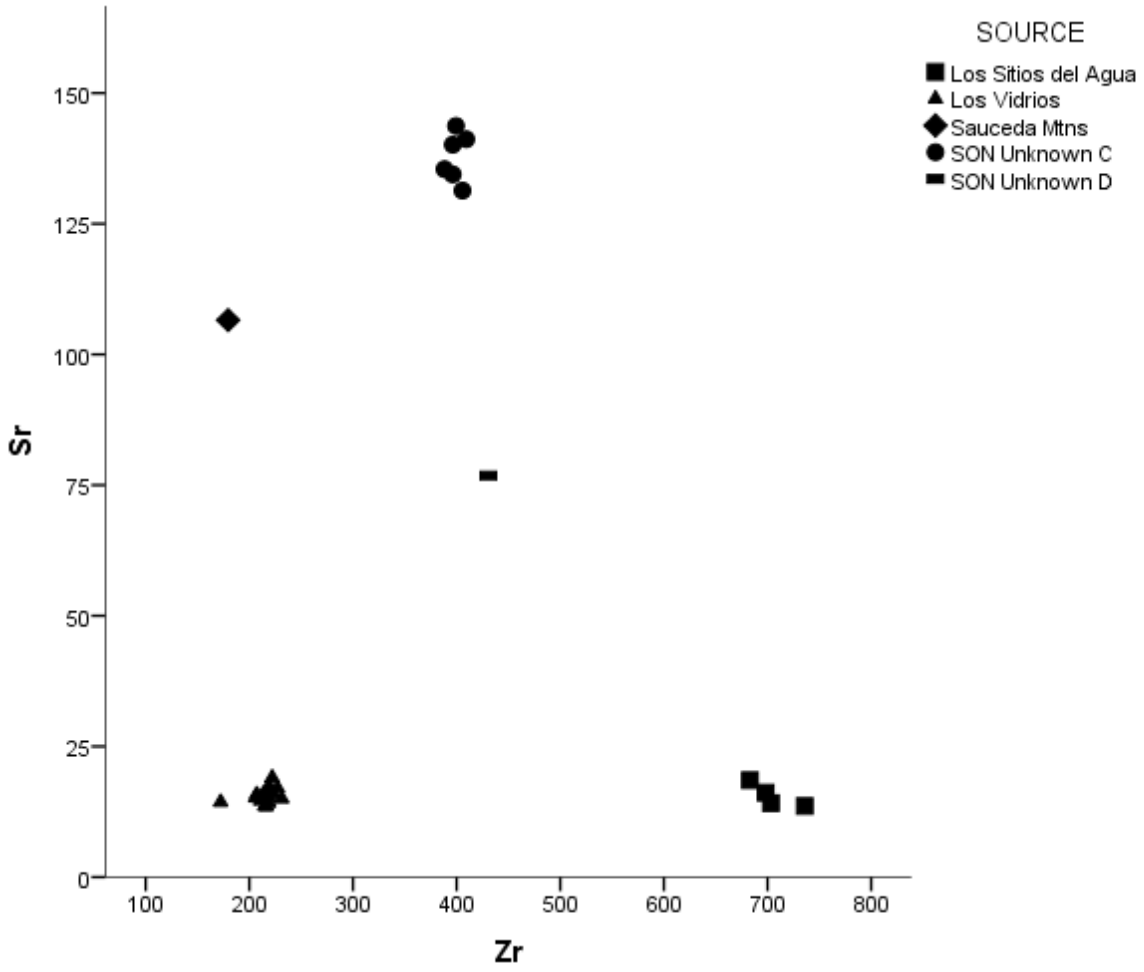

Figure 1. Zr versus Sr bivariate plot of the elemental concentrations for all the archaeological specimens from all sites.

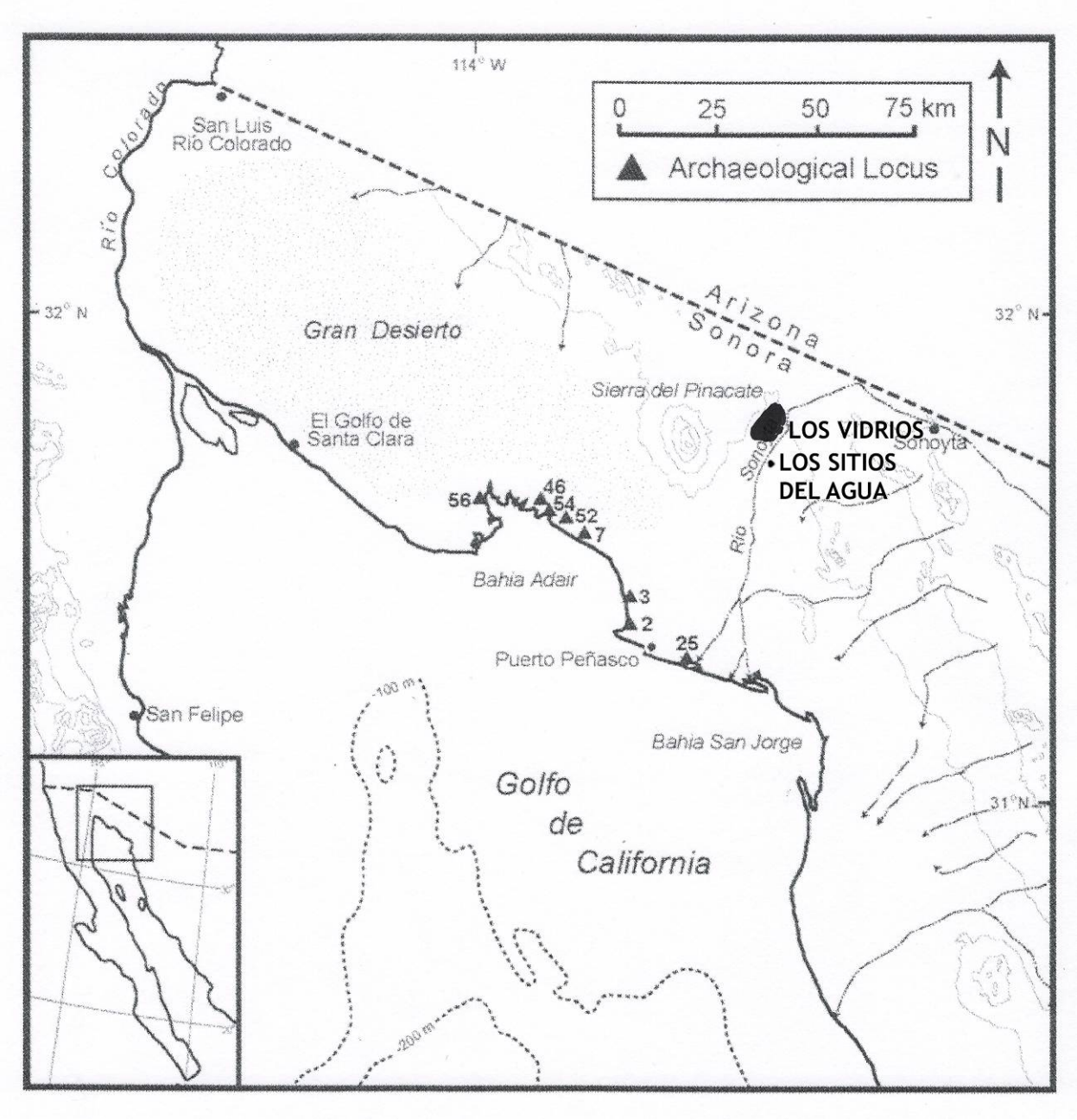

Figure 2. General location of the region, the approximate locations of the two dominant sources in northern Sonora, and the location of project sites (from Mitchell et. al. 2015).

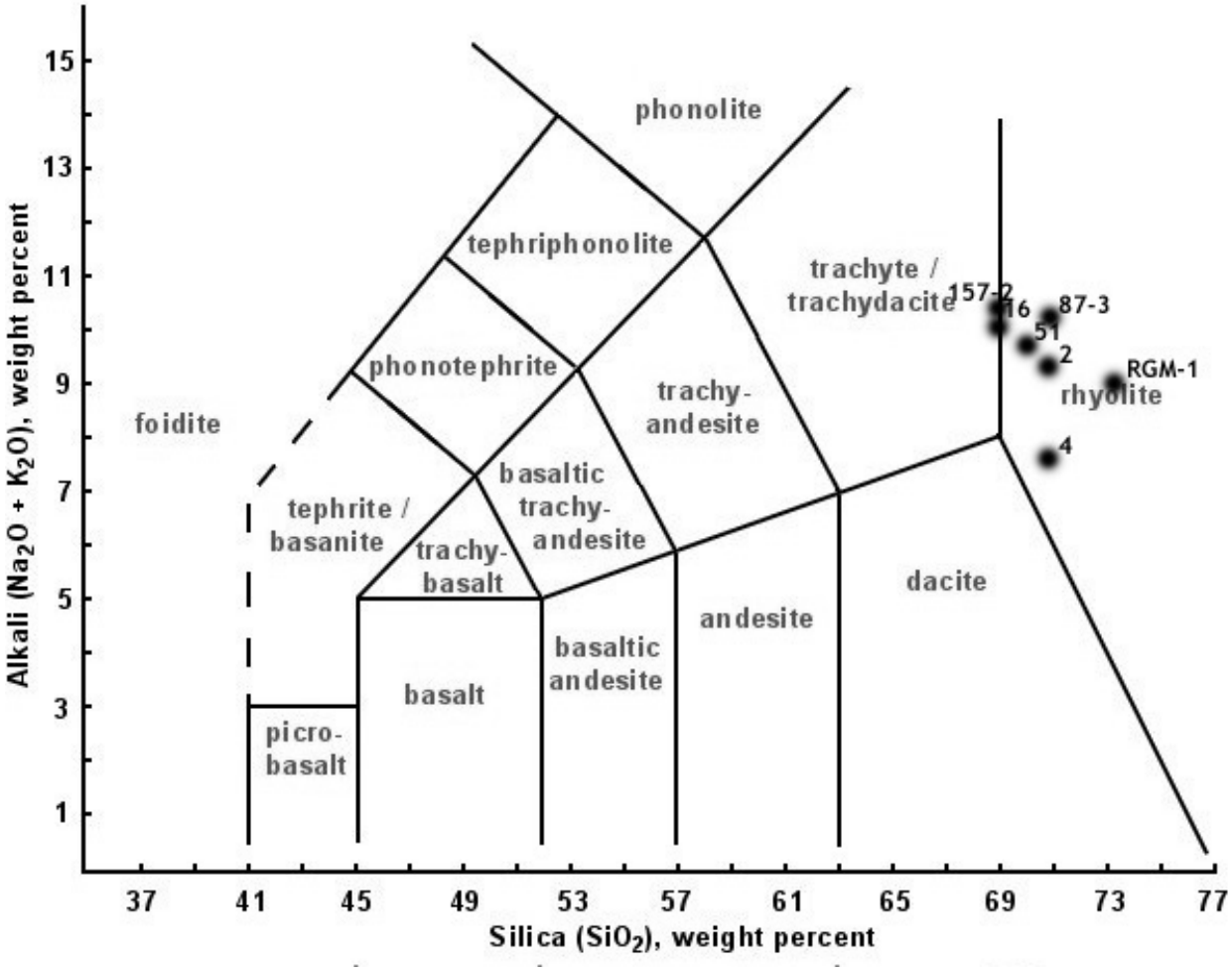

Figure 3. TAS plot of the "unknown" samples and RGM-1 USGS rhyolite standard.